C. R. Mecanique 346 (2018) 1123–1135

Contents lists available at ScienceDirect

Comptes Rendus Mecanique

www.sciencedirect.com

Designing isotropic composites reinforced by aligned transversely isotropic particles of spheroidal shape

Katell Derrien, Léo Morin *, Pierre Gilormini

PIMM, Arts et Métiers – ParisTech, CNAM, CNRS, 151, bd de l'Hôpital, 75013 Paris, France

ARTICLE INFO

Article history:
Received 22 June 2018
Accepted 25 September 2018
Available online 25 October 2018

Keywords:
Transverse isotropy
Spheroidal particles
Homogenization schemes
Composites

ABSTRACT

The aim of this paper is to study the design of isotropic composites reinforced by aligned spheroidal particles made of a transversely isotropic material. The problem is investigated analytically using the framework of mean-field homogenization. Conditions of macroscopic isotropy of particle-reinforced composites are derived for the dilute and Mori–Tanaka's schemes. This leads to a system of three nonlinear equations linking seven material constants and two geometrical constants. A design tool is finally proposed, which permits to determine admissible particles achieving macroscopic isotropy for a given isotropic matrix behavior and a given particle aspect ratio. Correlations between transverse and longitudinal moduli of admissible particles are studied for various particle shapes. Finally, the design of particles is investigated for aluminum and steel matrix composites.

1. Introduction

Composite materials constitute one of the most advanced class of materials whose popularity in industrial applications keeps growing exponentially [1]. Their advent has been aided by the development of new processing methods, theoretical approaches of homogenization [2,3] and numerical simulations of heterogeneous materials [4]. This class of materials is commonly divided into three categories [5]: (i) *fibrous composites* consisting of continuous fibers embedded in a matrix, (ii) *laminated composites* consisting of various stacked layers, and (iii) *particle-reinforced composites* composed of particles in a matrix. We are interested in this work in particle-reinforced composites, which cover a large range of existing materials, due to the various combinations of particles and matrices including notably concrete and polymer composites (nonmetallic particles in a nonmetallic matrix), solid-rocket propellants (metallic particles in nonmetallic matrix), and metal-matrix composites (nonmetallic particles in metallic matrix), as well as various manufacturing processes including powder metallurgy and eutectic solidification, among others.

The modeling of particle-reinforced composites can be tackled in a unified approach using homogenization techniques that are based on the distributions and the mechanical behaviors of the phases. Mean-field homogenization techniques are based on the concept of representative volume element together with appropriate averaging relations permitting to achieve a scale transition, known as the Hill–Mandel macrohomogeneity condition [6,7]. The determination of the overall behavior of linear composites can then be performed using either (i) *bounds*, as the rigorous first-order bounds of Voigt and Reuss on the effective moduli and the second-order bounds of Hashin and Shtrikman based on variational principles [8],

* Corresponding author.
E-mail address: leo.morin@ensam.eu (L. Morin).

https://doi.org/10.1016/j.crme.2018.09.004

or (ii) *estimates*, as the dilute scheme [9,10], Mori–Tanaka's scheme [11] and the generalized self-consistent scheme [12,13], which are all based on Eshelby's ellipsoidal inclusion problem [14].

In practical applications, reinforcements commonly induce anisotropy due to their crystalline orientation (material anisotropy) and their shape (morphological anisotropy). In the case of a hexagonal crystallographic symmetry, which covers a large range of materials, the material anisotropy reduces to transverse isotropy. Thus, in the quite general situation of aligned spheroidal transversely isotropic particles embedded in an isotropic matrix, it is natural to expect a transversely isotropic overall behavior when these two sources of anisotropy are combined. Unfortunately, the induced anisotropy restricts the possibilities of engineering composites because, in most of industrial applications, anisotropy is often seen as a drawback while macroscopic isotropy is pursued to simplify materials processing. However, one can wonder if the two sources of anisotropy (material and morphological) can cancel each other to lead to a macroscopic isotropic composite. This would permit to open new possibilities of engineering macroscopic composites made of anisotropic reinforcements. With the design of macroscopic isotropic enhanced composites in mind, it is thus of interest to understand the coupling between crystalline and particle-shape anisotropies and the conditions permitting to achieve macroscopic isotropy, in the framework of theoretical homogenization. The aim of this work is to provide a design tool for isotropic composites reinforced by aligned transversely isotropic particles. Section 2 presents the problem considered and notably the theoretical approach of mean-field homogenization. The condition of macroscopic isotropy is then derived in Section 3. Finally, a design tool is proposed in Section 4; correlations between transverse and longitudinal moduli of admissible particles are notably investigated.

2. Position of the problem

2.1. Preliminaries

We investigate the overall behavior of a two-phase composite made of an isotropic matrix reinforced by aligned transversely isotropic particles. The isotropic matrix is characterized by its shear and bulk moduli G_0 and K_0. The stiffness and compliance tensors of the matrix are denoted by $\mathbb{C}_0$ and $\mathbb{S}_0$, respectively. The volume fraction of the matrix is denoted by f_0. The particles are supposed to be transversely isotropic with stiffness and compliance tensors denoted by $\mathbb{C}_1$ and $\mathbb{S}_1$, respectively. The shape of the particles is assumed to be spheroidal with an aspect ratio w ($w<1$ corresponds to an oblate particle, $w=1$ spherical and $w>1$ prolate). Both material anisotropy and spheroidal axes are supposed to coincide with axis $\mathbf{e}_3$, so it is expected that the overall behavior is transversely isotropic. Finally, the volume fraction of the particle is denoted by $f_1=1-f_0$.

In order to derive the overall behavior of the composite, it will be useful to express elasticity tensors with Walpole formalism [15], which provides a convenient framework to manipulate transversely isotropic tensors[1]. Using this formalism, the transversely isotropic stiffness tensor $\mathbb{C}_1$ is given by

$$\mathbb{C}_1=[2k_1,\ l_1,\ n_1,\ 2m_1,\ 2p_1] \tag{1}$$

and the compliance tensor $\mathbb{S}_1$ reads

$$\mathbb{S}_1=\left[\frac{n_1}{2\Delta_1},\ -\frac{l_1}{2\Delta_1},\ \frac{k_1}{\Delta_1},\ \frac{1}{2m_1},\ \frac{1}{2p_1}\right] \tag{2}$$

where Δ_1 is given by

$$\Delta_1=k_1n_1-l_1^2 \tag{3}$$

Positive definiteness of $\mathbb{C}_1$ (and $\mathbb{S}_1$) requires that all k_1, m_1, p_1 and $n_1-l_1^2/k_1$ are positive [15]. The moduli k_1, l_1, n_1, m_1 and p_1 can be expressed in terms of the components $C_{1,ijkl}$ through the following relations:

$$\begin{cases} k_1 &= \dfrac{C_{1,1111}+C_{1,1122}}{2}=C_{1,1111}-C_{1,1212} \\ l_1 &= C_{1,1133}=C_{1,2233} \\ n_1 &= C_{1,3333} \\ m_1 &= C_{1,1212} \\ p_1 &= C_{1,2323}=C_{1,1313} \end{cases} \tag{4}$$

For practical reasons, it is also convenient to introduce the so-called *engineering* notations defining the transverse and longitudinal Young's moduli E_t and E_l, the transverse and longitudinal shear moduli G_t and G_l, and the longitudinal Poisson ratio ν_l. These coefficients are related to the moduli $(k_1,\ l_1,\ n_1,\ m_1,\ p_1)$ through

[1] Elements of Walpole formalism are recalled in Appendix A.

$$\begin{cases} E_{\mathrm{l}} &= n_1 - \dfrac{l_1^2}{k_1} \\ E_{\mathrm{t}} &= \dfrac{1}{\dfrac{1}{4k_1} + \dfrac{1}{4m_1} + \dfrac{1}{4\left(n_1 \dfrac{k_1^2}{l_1^2} - k_1\right)}} \\ G_{\mathrm{l}} &= p_1 \\ G_{\mathrm{t}} &= m_1 \\ \nu_{\mathrm{l}} &= \dfrac{l_1}{2k_1} \end{cases} \tag{5}$$

The isotropic stiffness tensor $\mathbb{C}_0$ can also be expressed in Walpole formalism:

$$\mathbb{C}_0 = [2k_0,\ l_0,\ n_0,\ 2m_0,\ 2p_0] \tag{6}$$

where

$$m_0 = p_0 = G_0, \quad k_0 = K_0 + \frac{1}{3}G_0,$$

$$l_0 = K_0 - \frac{2}{3}G_0, \quad n_0 = K_0 + \frac{4}{3}G_0$$

We finally recall that the Young's modulus E_0 and Poisson ratio ν_0 of the matrix are related to the bulk and shear moduli K_0 and G_0 through

$$E_0 = \frac{9K_0G_0}{3K_0 + G_0}, \quad \nu_0 = \frac{3K_0 - 2G_0}{2(3K_0 + G_0)} \tag{7}$$

2.2. Macroscopic behavior of a particle-reinforced composite

The effective behavior of the composite material is investigated by the mean-field approach of homogenization. Since classical homogenization schemes make intensive use of Eshelby's tensors, we recall that Eshelby's polarization tensor $\mathbb{P}$ (also known as Hill's tensor) obtained from the Eshelby (classical) tensor $\mathbb{S}^{\mathrm{esh}}$ [14] is given by

$$\mathbb{P} = \mathbb{S}^{\mathrm{esh}} : \mathbb{S}_0 \tag{8}$$

Tensor $\mathbb{P}$ depends on the moduli G_0 and K_0 of the matrix and on the aspect ratio w of the particle. It possesses the symmetry of a transversely isotropic tensor and thus can be written under the form

$$\mathbb{P} = \left[2k_{\mathrm{p}},\ l_{\mathrm{p}},\ n_{\mathrm{p}},\ 2m_{\mathrm{p}},\ 2p_{\mathrm{p}}\right] \tag{9}$$

where the expressions of coefficients k_{p}, l_{p}, n_{p}, m_{p} and p_{p} are given in Appendix B and have the physical dimension of a compliance.

First, we consider the dilute scheme [9,10], which applies for aligned ellipsoidal particles with a very small volume fraction. In its "primal" form, the macroscopic stiffness tensor, denoted by $\overline{\mathbb{C}}^{\mathrm{D}}$, is given by

$$\overline{\mathbb{C}}^{\mathrm{D}} = \mathbb{C}_0 + f_1 \left(\mathbb{P} + (\mathbb{C}_1 - \mathbb{C}_0)^{-1}\right)^{-1} \tag{10}$$

In its "dual" form, the macroscopic compliance tensor, denoted by $\overline{\mathbb{S}}^{\mathrm{D}}$, is given by

$$\overline{\mathbb{S}}^{\mathrm{D}} = \mathbb{S}_0 - f_1 \mathbb{S}_0 : \left(\mathbb{P} + (\mathbb{C}_1 - \mathbb{C}_0)^{-1}\right)^{-1} : \mathbb{S}_0 \tag{11}$$

It should be noted that $\overline{\mathbb{S}}^{\mathrm{D}} \neq \left(\overline{\mathbb{C}}^{\mathrm{D}}\right)^{-1}$, which means that the dilute scheme exhibits a "duality gap".

Then, we consider Mori–Tanaka's scheme [11], which applies for aligned ellipsoidal particles with a moderate volume fraction. For this model, the macroscopic stiffness tensor, denoted by $\overline{\mathbb{C}}^{\mathrm{MT}}$, is given by

$$\overline{\mathbb{C}}^{\mathrm{MT}} = \mathbb{C}_0 + f_1 \left(f_0 \mathbb{P} + (\mathbb{C}_1 - \mathbb{C}_0)^{-1}\right)^{-1} \tag{12}$$

Since Mori–Tanaka's scheme does not exhibit a "duality gap", the macroscopic compliance tensor $\overline{\mathbb{S}}^{\mathrm{MT}}$ simply reads $\overline{\mathbb{S}}^{\mathrm{MT}} = \left(\overline{\mathbb{C}}^{\mathrm{MT}}\right)^{-1}$.

In order to simplify the notations, the effective behavior of the composite, denoted by $\overline{\mathbb{C}}$, can thus be written under the generic form

$$\overline{\mathbb{C}} = \mathbb{C}_0 + f_1 \left(f_c \mathbb{P} + (\mathbb{C}_1 - \mathbb{C}_0)^{-1} \right)^{-1} \tag{13}$$

where $f_c = 1$ corresponds to the dilute scheme and $f_c = f_0$ corresponds to the model of Mori–Tanaka.

3. Condition of macroscopic isotropy

3.1. Generalities

The aim of this Section is to derive the conditions that the particle and the matrix must fulfill so that the macroscopic behavior given by Eq. (13) becomes isotropic. Obviously, from Eqs. (10), (11) and (12), a sufficient and necessary condition to ensure macroscopic isotropy is that the tensor

$$\mathbb{A} = f_c \mathbb{P} + (\mathbb{C}_1 - \mathbb{C}_0)^{-1} \tag{14}$$

is isotropic (since $\mathbb{C}_0$ and $\mathbb{S}_0$ are isotropic). It is interesting to note that the tensor $\mathbb{A}$ depends on (i) the coefficients of the isotropic matrix through $\mathbb{P}$ and $\mathbb{C}_0$, (ii) the anisotropy of the particles through $\mathbb{C}_1$ and (iii) the shape and volume fraction of the particle. Thus the condition of macroscopic isotropy will result in a subtle coupling between material anisotropy and shape of the particle.

3.2. Derivation of the isotropy condition

Using Walpole formalism, the tensor $\mathbb{A}$ reads

$$\mathbb{A} = \left[2 f_c k_p + \frac{n_1 - n_0}{2\Delta_A}, f_c l_p - \frac{l_1 - l_0}{2\Delta_A}, f_c n_p + \frac{k_1 - k_0}{\Delta_A}, 2 f_c m_p + \frac{1}{2(m_1 - m_0)}, 2 f_c p_p + \frac{1}{2(p_1 - p_0)} \right] \tag{15}$$

where Δ_A is given by

$$\Delta_A = (k_1 - k_0)(n_1 - n_0) - (l_1 - l_0)^2 \tag{16}$$

The isotropy condition implies that the tensor $\mathbb{A}$ must be written under the form

$$\mathbb{A} = [2(a+b),\ a,\ a+2b,\ 2b,\ 2b] \tag{17}$$

where a and b are arbitrary constants (see Appendix A). It should be noted that the parameters a and b are *not* related to a bulk modulus and a shear modulus, since the tensor $\mathbb{A}$ is not a stiffness tensor, but have the physical dimension of a compliance. Thus, the isotropy condition leads to the following system

$$\begin{cases} 2 f_c m_p + \dfrac{1}{2(m_1 - m_0)} & = 2 f_c p_p + \dfrac{1}{2(p_1 - p_0)} \\ 2 f_c k_p + \dfrac{n_1 - n_0}{2\Delta_A} & = 2 f_c l_p - \dfrac{l_1 - l_0}{\Delta_A} + 2 f_c p_p + \dfrac{1}{2(p_1 - p_0)} \\ f_c n_p + \dfrac{k_1 - k_0}{\Delta_A} & = f_c l_p - \dfrac{l_1 - l_0}{2\Delta_A} + 2 f_c p_p + \dfrac{1}{2(p_1 - p_0)} \end{cases} \tag{18}$$

The isotropy condition consists in a system of three equations linking nine parameters, seven material constants (K_0, G_0, k_1, l_1, n_1, m_1, p_1), one morphological constant (w), and a constant related to the volume fraction of particles (f_c).

It should be noted that in the case of the dilute scheme, corresponding to $f_c = 1$, the isotropy condition is independent of the volume fraction of reinforcements.

3.3. Macroscopic behavior

When the isotropy condition (18) is verified, it is possible to express the macroscopic stiffness tensor of the isotropic composite from Eq. (13), denoted by $\overline{\mathbb{C}}^{\text{iso}}$, in a very compact way:

$$\overline{\mathbb{C}}^{\text{iso}} = \left[2\left(\overline{K} + \frac{1}{3}\overline{G} \right),\ \overline{K} - \frac{2}{3}\overline{G},\ \overline{K} + \frac{4}{3}\overline{G},\ 2\overline{G},\ 2\overline{G} \right] \tag{19}$$

where

$$3\overline{K} = 3K_0 + f_1 \frac{1}{3c + 2d}, \quad 2\overline{G} = 2G_0 + f_1 \frac{1}{2d},$$

$$c = f_c l_p - \frac{l_1 - l_0}{2\Delta_A}, \quad d = f_c m_p + \frac{1}{4m_1 - m_0}$$

4. Design of transversely isotropic spheroidal particles achieving macroscopic isotropy

4.1. Generalities

The aim of this Section is to provide a design tool of transversely isotropic particles permitting to obtain macroscopic isotropic composites. Our objectives are twofold:

(1) we aim at providing analytic expressions of the components of the tensor $\mathbb{C}_1$ for a given matrix $\mathbb{C}_0$, a given shape w and a given volume fraction f_c of particles;
(2) we are interested in studying the correlation between material anisotropy through the coefficients of $\mathbb{C}_1$ and morphological anisotropy through the coefficients f_c and w.

The parameters K_0, G_0, f_c and w are thus assumed to be known and the problem reduces in finding the moduli k_1, l_1, n_1, m_1, p_1 that verify system (18). First, it is interesting to note that system (18) can be written under a dimensionless form by multiplying every terms by G_0; this leads to

$$\begin{cases} 2f_c G_0 m_p + \dfrac{1}{2\left(\dfrac{m_1}{G_0} - 1\right)} & = 2f_c G_0 p_p + \dfrac{1}{2\left(\dfrac{p_1}{G_0} - 1\right)} \\ 2f_c G_0 k_p + \dfrac{\dfrac{n_1}{G_0} - \dfrac{K_0}{G_0} - \dfrac{4}{3}}{2\tilde{\Delta}_A} & = 2f_c G_0 l_p - \dfrac{\dfrac{l_1}{G_0} - \dfrac{K_0}{G_0} + \dfrac{2}{3}}{\tilde{\Delta}_A} + 2f_c G_0 p_p + \dfrac{1}{2\left(\dfrac{p_1}{G_0} - 1\right)} \\ f_c G_0 n_p + \dfrac{\dfrac{k_1}{G_0} - \dfrac{K_0}{G_0} - \dfrac{1}{3}}{\tilde{\Delta}_A} & = f_c G_0 l_p - \dfrac{\dfrac{l_1}{G_0} - \dfrac{K_0}{G_0} + \dfrac{2}{3}}{2\tilde{\Delta}_A} + 2f_c G_0 p_p + \dfrac{1}{2\left(\dfrac{p_1}{G_0} - 1\right)} \end{cases} \tag{20}$$

where

$$\tilde{\Delta}_A = \left(\frac{k_1}{G_0} - \frac{K_0}{G_0} - \frac{1}{3}\right) \times \left(\frac{n_1}{G_0} - \frac{K_0}{G_0} - \frac{4}{3}\right) - \left(\frac{l_1}{G_0} - \frac{K_0}{G_0} + \frac{2}{3}\right)^2 \tag{21}$$

Here, the coefficients $G_0 k_p$, $G_0 l_p$, $G_0 n_p$, $G_0 m_p$ and $G_0 p_p$ are given by

$$\begin{cases} G_0 k_p & = \dfrac{7h(w) - 2w^2 - 4w^2 h(w) + \left(h(w) - 2w^2 + 2w^2 h(w)\right) 3K_0/G_0}{8(1 - w^2)\,(4 + 3K_0/G_0)} \\ G_0 l_p & = \dfrac{(2w^2 - h(w) - 2w^2 h(w)) \times (1 + 3K_0/G_0)}{4(1 - w^2)\,(4 + 3K_0/G_0)} \\ G_0 n_p & = \dfrac{6 - 5h(w) - 8w^2 h(w) + (h(w) - 2w^2 + 2w^2 h(w)) 3K_0/G_0}{2(1 - w^2)\,(4 + 3K_0/G_0)} \\ G_0 m_p & = \dfrac{15h(w) - 2w^2 - 12w^2 h(w) + (3h(w) - 2w^2) 3K_0/G_0}{16(1 - w^2)\,(4 + 3K_0/G_0)} \\ G_0 p_p & = \dfrac{8 - 6h(w) - 4w^2 + (2 - 3h(w) + 2w^2 - 3w^2 h(w)) 3K_0/G_0}{8(1 - w^2)\,(4 + 3K_0/G_0)} \end{cases} \tag{22}$$

where $h(w)$ is given in Appendix A.

The isotropy condition consists in a system of three equations that links the dimensionless moduli k_1/G_0, l_1/G_0, n_1/G_0, m_1/G_0, p_1/G_0 to w, f_c, and the ratio K_0/G_0. It is thus remarkable that these dimensionless ratios only depend on the matrix behavior through its Poisson ratio since the quantity K_0/G_0 reads, using Eq. (7):

$$\frac{3K_0}{G_0} = \frac{2(1+\nu_0)}{1-2\nu_0} \tag{23}$$

The resolution consists in finding five unknowns verifying three equations for which there are *a priori* an infinity of solutions. In order to determine a set of admissible material constants, it is however possible to fix arbitrarily two coefficients, n_1/G_0 and l_1/G_0 for instance, and to deduce the remaining three coefficients, which are given by

$$\begin{cases} \dfrac{k_1}{G_0} &= \dfrac{K_0}{G_0} + \dfrac{1}{3} + \dfrac{\dfrac{l_1}{G_0} + \dfrac{n_1}{G_0} - 2\dfrac{K_0}{G_0} - \dfrac{2}{3} - 2f_c(2G_0k_p - G_0l_p - G_0n_p)\left(\dfrac{l_1}{G_0} - \dfrac{K_0}{G_0} + \dfrac{2}{3}\right)^2}{2\left(1 - f_c(2G_0k_p - G_0l_p - G_0n_p)\left(\dfrac{n_1}{G_0} - \dfrac{K_0}{G_0} - \dfrac{4}{3}\right)^2\right)} \\ \dfrac{p_1}{G_0} &= 1 + \dfrac{\tilde{\Delta}_A}{\dfrac{n_1}{G_0} - 2\dfrac{l_1}{G_0} - 3\dfrac{K_0}{G_0} - 4f_c\tilde{\Delta}_A(G_0l_p + G_0p_p - G_0k_p)} \\ \dfrac{m_1}{G_0} &= 1 + \dfrac{\dfrac{p_1}{G_0} - 1}{1 + 4f_c\left(\dfrac{p_1}{G_0} - 1\right)(G_0p_p - G_0m_p)} \end{cases} \tag{24}$$

where $\tilde{\Delta}_A$ is given in terms of n_1/G_0 and l_1/G_0 using Eqs. (21) and $(24)_1$. Thus, if one explores accurately the space of n_1/G_0 and l_1/G_0, it is possible to obtain a large set of admissible values for the material constants and thus deduce the set of admissible particles for a given matrix behavior, shape, and volume fraction of particles.

4.2. Correlation between transverse and longitudinal shear moduli

First, we study the relation between transverse and longitudinal dimensionless shear moduli G_t/G_0 and G_l/G_0, which are given by

$$\begin{cases} \dfrac{G_t}{G_0} &= \dfrac{m_1}{G_0} \\ \dfrac{G_l}{G_0} &= \dfrac{p_1}{G_0} \end{cases} \tag{25}$$

where m_1/G_0 and p_1/G_0 are related to each other by Eq. $(24)_3$. Thus, the transverse shear modulus G_t/G_0 can be expressed in terms of the longitudinal shear modulus G_l/G_0 by the equation

$$\frac{G_t}{G_0} = 1 + \frac{\dfrac{G_l}{G_0} - 1}{1 + \left(\dfrac{G_l}{G_0} - 1\right) \times g\left(f_c, w, \dfrac{K_0}{G_0}\right)} \tag{26}$$

where the function $g\left(f_c, w, \dfrac{K_0}{G_0}\right)$ is given by

$$g\left(f_c, w, \frac{K_0}{G_0}\right) = f_c \frac{16 - 27h(w) - 6w^2 + 12h(w)w^2 + (4 - 9h(w) + 6w^2 - 6w^2h(w))3\dfrac{K_0}{G_0}}{4(1-w^2)\left(4 + 3\dfrac{K_0}{G_0}\right)} \tag{27}$$

It is remarkable that the shear moduli G_t/G_0 and G_l/G_0 of a particle achieving macroscopic isotropy are related to each other through a formula that only depends on the particle shape w, the ratio K_0/G_0 related to the Poisson ratio of the matrix, and the parameter f_c, which is related to the volume fraction f_0. For illustrative purpose, the transverse shear modulus G_t/G_0 versus the longitudinal shear modulus G_l/G_0 is represented in Fig. 1 for the value $f_c = 1$ (which corresponds to the dilute scheme), various values of the particle shape w, and various values of K_0/G_0 corresponding to different families of matrix materials: $K_0/G_0 = 1/6$ or $\nu_0 = -1/2$ (auxetic matrix), $K_0/G_0 = 4/3$ or $\nu_0 = 2/5$ (concrete), $K_0/G_0 = 8/3$ or $\nu_0 = 1/3$ (metallic alloys), $K_0/G_0 = 100$ or $\nu_0 = 0.495$ (rubber).

Some comments are in order.

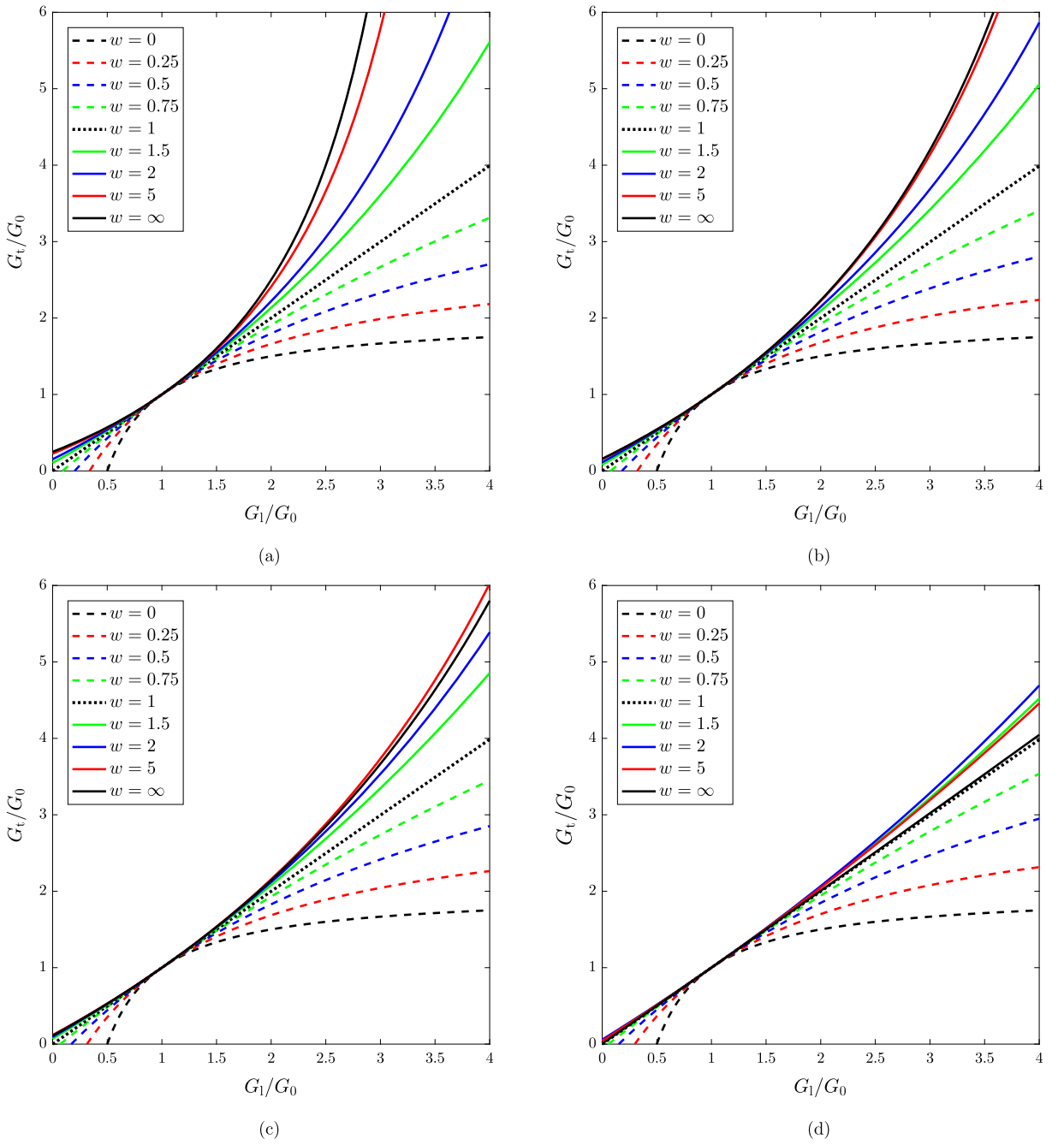

Fig. 1. Dimensionless transverse shear modulus G_t/G_0 versus longitudinal shear modulus G_l/G_0 in the case $f_c = 1$ (high dilution). (a) $K_0/G_0 = 1/6$ or $\nu_0 = -1/2$ (auxetic matrix), (b) $K_0/G_0 = 4/3$ or $\nu_0 = 2/5$ (concrete), (c) $K_0/G_0 = 8/3$ or $\nu_0 = 1/3$ (metallic alloys), and (d) $K_0/G_0 = 100$ or $\nu_0 = 0.495$ (rubber).

- For prolate particles ($w > 1$), the transverse shear modulus of a particle achieving macroscopic isotropy is greater than the longitudinal shear modulus. Thus, the morphological anisotropy induced by the particle shape is balanced by an increase of the transverse shear modulus. In the asymptotic geometrical case $w \to +\infty$ corresponding to fibers, Eq. (26) reduces to

$$\frac{G_t}{G_0} = 1 + \frac{\dfrac{G_l}{G_0} - 1}{1 - \dfrac{3f_c}{2(4 + 3K_0/G_0)} \times \left(\dfrac{G_l}{G_0} - 1\right)} \tag{28}$$

It is thus possible to achieve macroscopic isotropy with parallel anisotropic cylindrical fibers, but their shear modulus is limited by the value

$$\left(\frac{G_l}{G_0}\right)_{\max} = 1 + \frac{2}{3f_c}\left(4 + 3K_0/G_0\right) \tag{29}$$

- For spherical particles ($w = 1$), one gets $g = 0$ and thus $G_t = G_l$. This is of course expected since in this case, the only way to achieve macroscopic isotropy is to consider isotropic particles.
- For oblate particles ($w < 1$), the transverse shear modulus of a particle achieving macroscopic isotropy is lower than the longitudinal shear modulus. Again, the morphological anisotropy induced by the particle shape is balanced by an increase of material anisotropy. In the asymptotic case $w \to 0$ corresponding to penny shape particles, Eq. (26) reduces to

$$\frac{G_t}{G_0} = 1 + \frac{\dfrac{G_l}{G_0} - 1}{1 + f_c\left(\dfrac{G_l}{G_0} - 1\right)} \tag{30}$$

Thus, it is also possible to achieve macroscopic isotropy with parallel penny shape particles, but their transverse shear modulus is limited by the value

$$\left(\frac{G_t}{G_0}\right)_{\max} = 1 + \frac{1}{f_c} \tag{31}$$

4.3. Correlation between transverse and longitudinal Young's moduli

We study now the correlation between transverse and longitudinal Young's moduli. From Eq. (5), the dimensionless transverse and longitudinal Young's moduli E_t/E_0 and E_l/E_0 are given by

$$\begin{cases} \dfrac{E_l}{E_0} = \left(\dfrac{9K_0/G_0}{3K_0/G_0 + 1}\right)\left(\dfrac{n_1}{G_0} - \left(\dfrac{l_1}{G_0}\right)^2 \dfrac{G_0}{k_1}\right) \\ \dfrac{E_t}{E_0} = \dfrac{36K_0/G_0}{3K_0/G_0 + 1} \times \dfrac{1}{\dfrac{G_0}{k_1} + \dfrac{G_0}{m_1} + \dfrac{1}{\dfrac{n_1}{G_0}\left(\dfrac{k_1}{G_0}\right)^2\left(\dfrac{G_0}{l_1}\right)^2 - \dfrac{k_1}{G_0}}} \end{cases} \tag{32}$$

where the coefficients k_1/G_0 and m_1/G_0 are given in terms of n_1/G_0 and l_1/G_0 by Eq. (24). It appears that the transverse and longitudinal Young's moduli are both expressed only in terms of n_1/G_0 and l_1/G_0 in a very nonlinear way. In contrast to the case of the shear moduli studied in Section 4.2, it is impossible to obtain an analytic relation between E_t/E_0 and E_l/E_0 involving only f_c, w and K_0/G_0. However, it is still possible to determine a set of admissible values E_l/E_0 and E_t/E_0 by exploring the space of n_1/G_0 and l_1/G_0 as explained in Section 4.1. A large number of values is considered, which permits to plot in Fig. 2 the ratio E_t/E_0 versus E_l/E_0 for the same K_0/G_0 values as in Fig. 1. Again, the value $f_c = 1$ is considered in all cases.

Overall, the results are similar to those obtained for the shear moduli, in particular for $K_0/G_0 = 4/3$ and $K_0/G_0 = 8/3$. It is worth noting that the relation between the transverse and longitudinal moduli is no longer a bijection: for a given value E_l/E_0, there are multiple admissible values E_t/E_0 that are bounded, the size of the domain depending on the values of w and K_0/G_0. For prolate particles achieving macroscopic isotropy, the transverse Young's modulus is in general greater than the longitudinal one. Conversely, for oblate particles achieving macroscopic isotropy, the transverse Young's modulus is in general lower than the longitudinal one. It should be noted that peculiar behaviors are observed mainly for a rubber matrix ($K_0/G_0 = 100$ or $\nu_0 = 0.495$), where the transverse Young's modulus can be lower than the longitudinal one for prolate particles and the transverse Young's modulus greater than the longitudinal one for oblate particles. These peculiar behaviors are notably due to admissible materials that possess a negative transverse Poisson ratio given by $\nu_t = E_t/(2G_t) - 1$.

4.4. Application to metal-matrix composites

We investigate finally the design of particles for aluminum and steel matrix composites, and notably their possible relation with popular particles such as silicon carbide (SiC) and titanium diboride (TiB_2).

If it is unlikely that a 9-tuplets (K_0, G_0, k_1, l_1, n_1, m_1, p_1, w, f_c) could lead to macroscopic isotropy in the exact case of Al–SiC and Fe–TiB_2 composites, it is however possible to determine admissible materials constituting the particles achieving macroscopic isotropy, called *ideal materials*, which are close to the desired materials (SiC or TiB_2), called *real materials*. The closeness between real and ideal materials is characterized by the distance between their stiffness tensors, denoted by $\mathbb{C}_{\text{real}}$

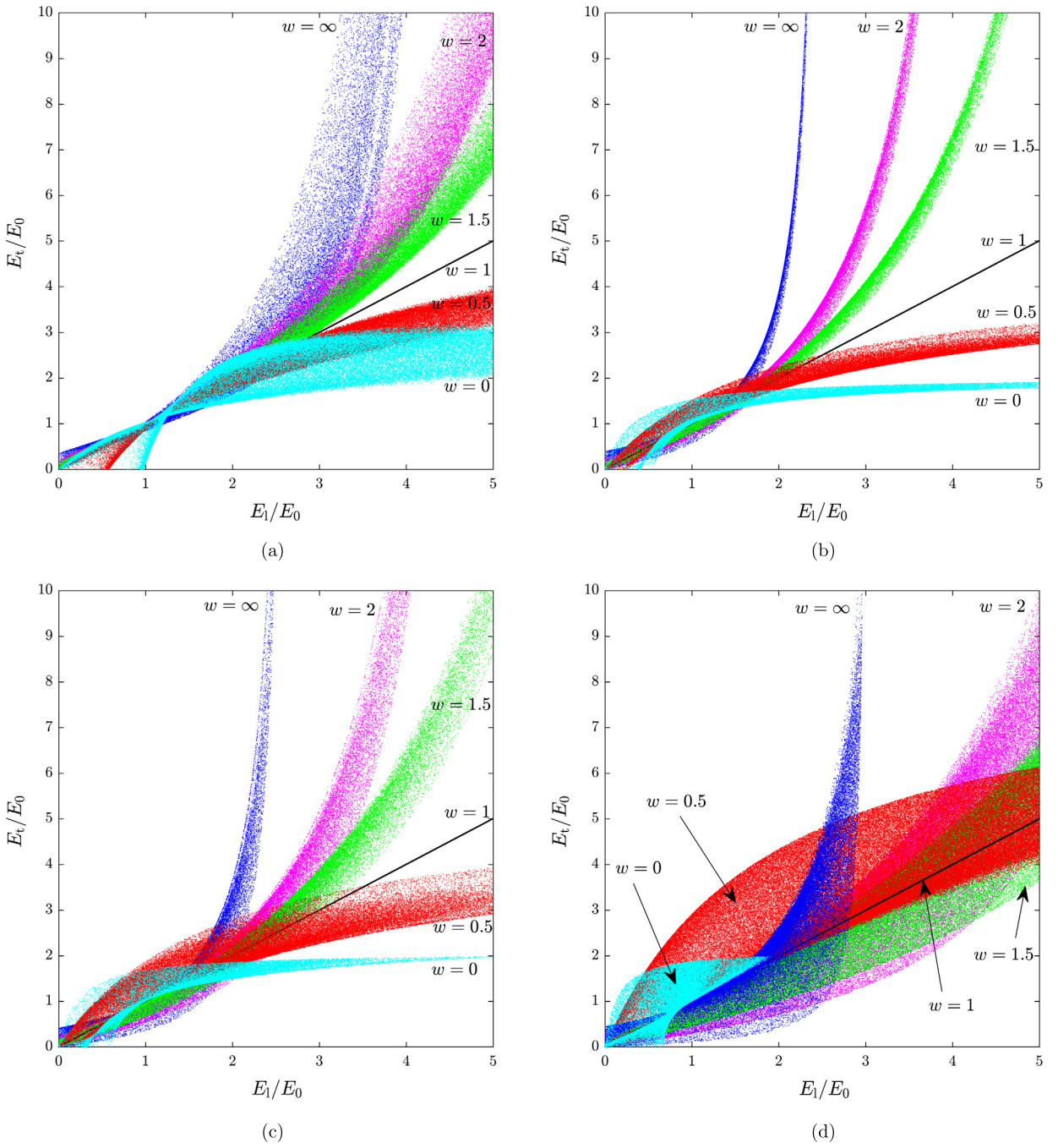

Fig. 2. Dimensionless transverse Young's modulus E_t/E_0 versus longitudinal Young's modulus E_l/E_0 in the case $f_c = 1$ (high dilution). (a) $K_0/G_0 = 1/6$ or $\nu_0 = -1/2$ (auxetic matrix), (b) $K_0/G_0 = 4/3$ or $\nu_0 = 2/5$ (concrete), (c) $K_0/G_0 = 8/3$ or $\nu_0 = 1/3$ (metallic alloys), and (d) $K_0/G_0 = 100$ or $\nu_0 = 0.495$ (rubber).

and $\mathbb{C}_{\text{ideal}}$, respectively. The Log-Euclidean distance [16,17] is used in order to provide a relative error between tensors, denoted by $\text{dist}(\mathbb{C}_{\text{real}}, \mathbb{C}_{\text{ideal}})$ and given by:

$$\text{dist}(\mathbb{C}_{\text{real}}, \mathbb{C}_{\text{ideal}}) = \frac{||\log(\mathbb{C}_{\text{real}}) - \log(\mathbb{C}_{\text{ideal}})||}{\sqrt{6}} \tag{33}$$

The procedure to obtain the logarithm of a matrix can be found in [16]. The choice of the Log-Euclidean distance over the classical Euclidean distance is motivated by the fact that it preserves the invariance under the operation of inversion and thus the duality between stiffness and compliance [16,17]. It should be noted that the coefficient $\sqrt{6}$ in Eq. (33) has been

Table 1
Closest materials to a real 6H–SiC [20] achieving macroscopic isotropy for various aspect ratios w. The elastic moduli C_{ijkl}, E_l, E_t, G_l and G_t are expressed in GPa.

Material	C_{1111}	C_{1122}	C_{1133}	C_{3333}	C_{2323}	E_l	E_t	G_l	G_t	ν_l	dist.
6H–SiC Case 1 [20]	498	186	176	567	141	476	404	141	156	0.257	–
Ideal particle											
$f_1 = 0.1$, $w = 0.5$	333	140	186	685	168	538	254	168	96	0.39	0.354
$f_1 = 0.1$, $w = 0.8$	447	178	192	595	164	477	350	164	134	0.31	0.136
$f_1 = 0.1$, $w = 0.9$	478	186	191	546	160	435	376	160	146	0.29	0.096
$f_1 = 0.1$, $w = 0.96$	492	189	191	517	157	410	388	157	151	0.28	0.091
$f_1 = 0.1$, $w = 2$	544	177	188	331	125	233	426	125	184	0.26	0.311

Table 2
Closest materials to a real 6H–SiC [21] achieving macroscopic isotropy for various aspect ratios w. The elastic moduli C_{ijkl}, E_l, E_t, G_l, and G_t are expressed in GPa.

Material	C_{1111}	C_{1122}	C_{1133}	C_{3333}	C_{2323}	E_l	E_t	G_l	G_t	ν_l	dist.
6H–SiC Case 2 [21]	501	111	52	553	163	544	473	163	195	0.085	–
Ideal particle											
$f_1 = 0.1$, $w = 0.5$	298	87	82	625	212	590	267	212	106	0.21	0.441
$f_1 = 0.1$, $w = 0.8$	416	101	86	573	204	544	384	204	158	0.17	0.203
$f_1 = 0.1$, $w = 0.9$	449	98	89	522	198	493	418	198	175	0.16	0.157
$f_1 = 0.1$, $w = 0.97$	471	97	94	492	194	461	439	194	187	0.17	0.145
$f_1 = 0.1$, $w = 2$	526	43	118	295	146	246	479	146	241	0.21	0.375

added to the classical Log-Euclidean distance so that the distance between two tensors $\mathbb{C}_1$ and $\alpha\mathbb{C}_1$, with α a non-negative scalar, reduces to $\mathrm{dist}(\mathbb{C}_1, \alpha\mathbb{C}_1) = \log(\alpha)$; this permits to extend the notion of "relative error" to the tensorial case.

Case of Al–SiC First, we consider the case of an aluminum matrix ($E_0 = 68.8$ GPa, $G_0 = 26$ GPa, $\nu_0 = 0.32$) reinforced by silicon carbide particles (Al–SiC), which constitutes one of the most popular metal-matrix composites due to an increase of tensile strength, hardness and wear resistance [18]. Silicon carbides can be found under various polytypes (cubic, hexagonal, or rhombohedral) inducing various elastic behaviors, according to the Landolt–Bornstein database. We consider here the 6H–SiC polytype, which is the most commonly used SiC polytype [19], for which there are several existing sets of elastic constants in the literature. We consider two sets of elastic constants, obtained from (i) a bond charge model calculation [20] (case 1) and (ii) Brillouin scattering experiments [21] (case 2). The stiffness tensors obtained from these two approaches are slightly different (see Tables 1 and 2), and the relative error between these two tensors takes the value

$$\mathrm{dist}(\mathbb{C}_{\mathrm{real}}^{\mathrm{case1}}, \mathbb{C}_{\mathrm{real}}^{\mathrm{case2}}) = 0.231 \tag{34}$$

This value permits to express the degree of uncertainty that is made on the knowledge of the material behavior. The elastic constants of the closest ideal particles achieving macroscopic isotropy, together with the associated relative errors, are given for various particle shapes in Tables 1 and 2, for the cases 1 and 2 respectively. For the case 1, it is possible to achieve isotropy with a material reasonably close to the real 6H–SiC [20] for $f_1 = 0.1$ and $w = 0.96$, with a distance that takes the value 0.091. For the case 2, it is possible to achieve isotropy with a material also reasonably close to the second real 6H–SiC [21] for $f_1 = 0.1$ and $w = 0.97$, with a distance that takes this time the value 0.145. Thus, in both cases, it is possible to achieve macroscopic isotropy with slightly oblate particles made of materials that are close to real SiC, with a relative error that is of the order of the uncertainty made on the SiC constants.

Case of Fe–TiB$_2$ Then, we consider the case of a steel ($E_0 = 208$ GPa, $G_0 = 80$ GPa, $\nu_0 = 0.3$) reinforced by titanium diboride (Fe–TiB$_2$), which is a promising material with improved specific properties [22]. As in the case of SiC, there are several sets of elastic constants available in the literature. We consider two sets obtained from (i) the pulse-echo method [23] (case 3), (ii) the rectangular parallelepiped resonance method [24] (case 4). The associated stiffness tensors are again quite different (see Tables 3 and 4), and their distance takes the value

$$\mathrm{dist}(\mathbb{C}_{\mathrm{real}}^{\mathrm{case3}}, \mathbb{C}_{\mathrm{real}}^{\mathrm{case4}}) = 0.556 \tag{35}$$

The elastic constants of the closest ideal particles achieving macroscopic isotropy, together with the associated relative errors, are given for various particle shapes in Tables 3 and 4, for the cases 3 and 4 respectively. For the case 3, it is possible to achieve isotropy with a material reasonably close to the real TiB$_2$ [23] for $f_1 = 0.1$ and $w = \infty$, with a distance that takes the value 0.312. For the case 4, it is possible to achieve isotropy with a material very close to the second real TiB$_2$ [24] for $f_1 = 0.1$ and $w = 4$, with a distance that takes this time the value 0.066. Thus, in both cases, it is possible to achieve

Table 3
Closest materials to a real TiB_2 [23] achieving macroscopic isotropy for various aspect ratios w. The elastic moduli C_{ijkl}, E_l, E_t, G_l, and G_t are expressed in GPa.

Material	C_{1111}	C_{1122}	C_{1133}	C_{3333}	C_{2323}	E_l	E_t	G_l	G_t	ν_l	dist.
TiB_2 Case 3 [23]	690	410	320	440	250	254	389	250	140	0.29	–
Ideal particle											
$f_1 = 0.1$, $w = 0.5$	593	276	298	692	176	487	417	176	158	0.34	0.353
$f_1 = 0.1$, $w = 1.5$	682	338	327	630	165	420	457	165	172	0.32	0.337
$f_1 = 0.1$, $w = 2$	682	333	319	604	165	404	461	165	175	0.31	0.333
$f_1 = 0.1$, $w = 5$	703	343	324	577	166	376	471	166	180	0.31	0.321
$f_1 = 0.1$, $w = \infty$	714	342	325	565	171	366	482	171	186	0.31	0.312

Table 4
Closest materials to a real TiB_2 [24] achieving macroscopic isotropy for various aspect ratios w. The elastic moduli C_{ijkl}, E_l, E_t, G_l, and G_t are expressed in GPa.

Material	C_{1111}	C_{1122}	C_{1133}	C_{3333}	C_{2323}	E_l	E_t	G_l	G_t	ν_l	dist.
TiB_2 Case 4 [24]	660	48	93	432	260	408	639	260	306	0.13	–
Ideal particle											
$f_1 = 0.1$, $w = 0.5$	519	90	51	614	278	605	501	278	215	0.08	0.274
$f_1 = 0.1$, $w = 1.5$	627	54	89	556	255	532	610	255	287	0.13	0.116
$f_1 = 0.1$, $w = 2$	637	37	96	527	252	499	619	252	300	0.14	0.088
$f_1 = 0.1$, $w = 4$	643	22	113	485	247	446	617	247	310	0.17	0.066
$f_1 = 0.1$, $w = \infty$	645	9	124	458	252	411	611	252	318	0.19	0.074

macroscopic isotropy with elongated particles made of materials that are close to TiB_2 with a relative error that is smaller than the uncertainty made on TiB_2 elastic constants.

5. Conclusion

The aim of this paper was to study the design of isotropic composites made of an isotropic matrix reinforced by aligned transversely isotropic particles of spheroidal shape.

First, we derived analytical conditions for macroscopic isotropy of composites reinforced by aligned transversely isotropic particles of spheroidal shape in the framework of mean-field homogenization using the dilute and Mori–Tanaka's schemes. This has permitted to express the isotropy condition as a system of three nonlinear equations liking nine parameters. Sets of admissible anisotropic particles were then provided for a given matrix behavior and shape of the particles. Correlations between transverse and shear moduli have permitted to investigate the coupling between material and morphological anisotropies. In general, the transverse modulus is greater than the longitudinal modulus for prolate particles. Conversely, the transverse modulus is in general lower than the longitudinal modulus for oblate particles. Finally, the design of metal-matrix composite was investigated. In the case of an aluminum matrix, admissible oblate particles close to SiC have been found to achieve macroscopic isotropy, permitting the design of isotropic Al–SiC composites. In the case of a steel matrix, admissible elongated particles close to TiB_2 have been found to achieve macroscopic isotropy, permitting the design of isotropic Fe–TiB_2 composites.

The obtained design may be directly used in industrial applications to provide new isotropic composites made of standard, anisotropic reinforcements such as SiC or TiB_2, for instance. Interestingly, it could be also employed in more complicated situations where the mechanical properties are designed to be isotropic, but other physical properties, such as electrical or acoustic properties, may stay anisotropic due to the particle shape.

Finally, it should be noted that the design tool proposed in this paper only applies to some ideal situations. In order to extend this design to more realistic situations, several directions can be explored.

- The spatial distribution of the particles' centers, which was supposed to be random, could be introduced in order to account for a more realistic microstructure. The effect of spatial distribution was investigated, in the theoretical homogenization framework, by Ponte Castañeda and Willis [25] through a distribution tensor that modifies Mori–Tanaka's estimate. Thus, it would be possible to derive a condition of macroscopic isotropy including this effect (at the cost of additional parameters).
- Particles were supposed to be perfectly aligned and material anisotropy axes of the particles were supposed to coincide with the geometric anisotropy axes; these assumptions permitted to obtain a first estimate of the parameters achieving macroscopic isotropy. It could be interesting to complement the proposed approximate design by full-field simulations performed on real microstructures in order to investigate the effect of these assumptions on macroscopic isotropy.

Acknowledgements

Fruitful discussions with Z. Hamouche are gratefully acknowledged.

Appendix A. Walpole formalism

Walpole formalism [15] is a convenient framework to manipulate transversely isotropic fourth-order tensors. Let us consider two transversely isotropic tensors given by

$$\mathbb{L}_1 = [2k_1,\ l_1,\ n_1,\ 2m_1,\ 2p_1], \qquad \mathbb{L}_2 = [2k_2,\ l_2,\ n_2,\ 2m_2,\ 2p_2] \tag{36}$$

The product between $\mathbb{L}_1$ and $\mathbb{L}_2$ is given by

$$\mathbb{L}_1 : \mathbb{L}_2 = [4k_1k_2 + 2l_1l_2,\ 2k_1l_2 + n_2l_1,\ 2l_1l_2 + n_1n_2,\ 4m_1m_2,\ 4p_1p_2] \tag{37}$$

and the inverse of $\mathbb{L}_1$ is given by

$$\mathbb{L}_1^{-1} = \left[\frac{n_1}{2\Delta_1},\ -\frac{l_1}{2\Delta_1},\ \frac{k_1}{\Delta_1},\ \frac{1}{2m_1},\ \frac{1}{2p_1}\right], \quad \Delta_1 = k_1n_1 - l_1^2 \tag{38}$$

An isotropic stiffness tensor $\mathbb{C}_{\text{iso}}$, with bulk and shear moduli denoted by K_{iso} and G_{iso}, respectively, can be written under the form

$$\mathbb{C}_{\text{iso}} = [2(\alpha+\beta),\ \alpha,\ \alpha+2\beta,\ 2\beta,\ 2\beta] \tag{39}$$

where

$$\beta = G_{\text{iso}}, \quad \alpha = K_{\text{iso}} - \frac{2}{3}G_{\text{iso}} \tag{40}$$

The corresponding isotropic compliance tensor $\mathbb{S}_{\text{iso}} = \mathbb{C}_{\text{iso}}^{-1}$ can also be written under the form

$$\mathbb{S}_{\text{iso}} = [2(\gamma+\delta),\ \gamma,\ \gamma+2\delta,\ 2\delta,\ 2\delta] \tag{41}$$

where

$$\delta = \frac{1}{4\beta} = \frac{1}{4G_{\text{iso}}}, \quad \gamma = \frac{1}{9\alpha+6\beta} - \frac{1}{6\beta} = \frac{1}{9K_{\text{iso}}} - \frac{1}{6G_{\text{iso}}} \tag{42}$$

Appendix B. Eshelby polarization tensor

The components of the Eshelby polarization tensor $\mathbb{P}$ for a spheroidal inclusion with aspect ratio w and axis of symmetry $\mathbf{e}_3$ embedded in an isotropic matrix with shear and bulk moduli G_0 and K_0 are given, in Walpole formalism, by [25]

$$\begin{cases} k_p &= \dfrac{\left(7h(w) - 2w^2 - 4w^2h(w)\right)G_0 + 3\left(h(w) - 2w^2 + 2w^2h(w)\right)K_0}{8(1-w^2)G_0(4G_0+3K_0)} \\ l_p &= \dfrac{(2w^2 - h(w) - 2w^2h(w))(G_0+3K_0)}{8(1-w^2)G_0(4G_0+3K_0)} \\ n_p &= \dfrac{(6 - 5h(w) - 8w^2h(w))G_0 + 3(h(w) - 2w^2 + 2w^2h(w))K_0}{2(1-w^2)G_0(4G_0+3K_0)} \\ m_p &= \dfrac{(15h(w) - 2w^2 - 12w^2h(w))G_0 + 3(3h(w) - 2w^2)K_0}{16(1-w^2)G_0(4G_0+3K_0)} \\ p_p &= \dfrac{2(4 - 3h(w) - 2w^2)G_0 + 3(2 - 3h(w) + 2w^2 - 3w^2h(w))K_0}{8(1-w^2)G_0(4K_0+3K_0)} \end{cases} \tag{43}$$

For oblate spheroids ($w < 1$), the function h is given by

$$h(w) = \frac{w\left(\arccos(w) - w\sqrt{w^2-1}\right)}{(1-w^2)^{\frac{3}{2}}} \tag{44}$$

and for prolate spheroids ($w > 1$), it reads

$$h(w) = \frac{w\left(w\sqrt{w^2-1} - \operatorname{argcosh}(w)\right)}{(w^2-1)^{\frac{3}{2}}} \tag{45}$$

The limit $w \to 1$ gives $h(1) = 2/3$ for a sphere.

References

[1] D. Gay, Composite Materials: Design and Applications, third edition, CRC Press, 2014.
[2] P. Ponte Castañeda, P. Suquet, Nonlinear composites, Adv. Appl. Mech. 34 (1997) 171–302.
[3] G.W. Milton, The Theory of Composites, Cambridge University Press, 2002.
[4] H. Moulinec, P. Suquet, A numerical method for computing the overall response of nonlinear composites with complex microstructure, Comput. Methods Appl. Mech. Eng. 157 (1998) 69–94.
[5] R.M. Jones, Mechanics of Composite Materials, CRC Press, 1998.
[6] J. Mandel, Contribution théorique à l'étude de l'écrouissage et des lois de l'écoulement plastique, in: Proceedings of the 11th International Congress on Applied Mechanics, Munich, Germany, 1964, pp. 502–509.
[7] R. Hill, The essential structure of constitutive laws for metal composites and polycrystals, J. Mech. Phys. Solids 15 (1967) 79–95.
[8] Z. Hashin, S. Shtrikman, A variational approach to the theory of the elastic behaviour of multiphase materials, J. Mech. Phys. Solids 11 (1963) 127–140.
[9] J.R. Willis, Elasticity theory of composites, in: Mechanics of Solids, Pergamon, Oxford, UK, 1982, pp. 653–686.
[10] Y. Benveniste, A new approach to the application of Mori–Tanaka's theory in composite materials, Mech. Mater. 6 (1987) 147–157.
[11] T. Mori, K. Tanaka, Average stress in matrix and average elastic energy of materials with misfitting inclusions, Acta Metall. 21 (1973) 571–574.
[12] R. Hill, A self-consistent mechanics of composite materials, J. Mech. Phys. Solids 13 (1965) 213–222.
[13] R.M. Christensen, K.H. Lo, Solutions for effective shear properties in three phase sphere and cylinder models, J. Mech. Phys. Solids 27 (1979) 315–330.
[14] J.D. Eshelby, The determination of the elastic field of an ellipsoidal inclusion, and related problems, Proc. R. Soc. Lond. A 241 (1957) 376–396.
[15] L.J. Walpole, On the overall elastic moduli of composite materials, J. Mech. Phys. Solids 17 (1969) 235–251.
[16] V. Arsigny, P. Fillard, X. Pennec, N. Ayache, Log-Euclidean metrics for fast and simple calculus on diffusion tensors, Magn. Reson. Med. 56 (2006) 411–421.
[17] M. Moakher, A.N. Norris, The closest elastic tensor of arbitrary symmetry to an elasticity tensor of lower symmetry, J. Elast. 85 (2006) 215–263.
[18] I.A. Ibrahim, F.A. Mohamed, E.J. Lavernia, Particulate reinforced metal matrix composites — a review, J. Mater. Sci. 26 (1991) 1137–1156.
[19] S. Adachi, Optical Constants of Crystalline and Amorphous Semiconductors: Numerical Data and Graphical Information, Springer Science & Business Media, 1999.
[20] M. Hofmann, A. Zywietz, K. Karch, F. Bechstedt, Lattice dynamics of SiC polytypes within the bond-charge model, Phys. Rev. B 50 (1994) 13401–13411.
[21] K. Kamitani, M. Grimsditch, J.C. Nipko, C.-K. Loong, M. Okada, I. Kimura, The elastic constants of silicon carbide: a Brillouin-scattering study of 4H and 6H SiC single crystals, J. Appl. Phys. 82 (1997) 3152–3154.
[22] Z. Hadjem-Hamouche, K. Derrien, E. Héripré, J.-P. Chevalier, In-situ experimental and numerical studies of the damage evolution and fracture in a Fe–TiB_2 composite, Mater. Sci. Eng. A 724 (2018) 594–605.
[23] J.J. Gilman, B.W. Roberts, Elastic constants of TiC and TiB_2, J. Appl. Phys. 32 (1961) 1405.
[24] N.L. Okamoto, M. Kusakari, K. Tanaka, H. Inui, S. Otani, Anisotropic elastic constants and thermal expansivities in monocrystal CrB_2, TiB_2, and ZrB_2, Acta Mater. 58 (2010) 76–84.
[25] P. Ponte Castañeda, J.R. Willis, The effect of spatial distribution on the effective behavior of composite materials and cracked media, J. Mech. Phys. Solids 43 (1995) 1919–1951.